Synthesis and Characterization of Hyperbranched Polyethylenes Tethered with Polyhedral Oligomeric Silsesquioxane (POSS) Nanoparticles by Chain Walking Ethylene Copolymerization with Acryloisobutyl-POSS

Jianli Wang,[†] Zhibin Ye,*[,†] and Helen Joly[‡]

School of Engineering, Laurentian University, Sudbury, Ontario, Canada P3E 2C6, and Department of Chemistry and Biochemistry, Laurentian University, Sudbury, Ontario, Canada P3E 2C6

Received March 20, 2007; Revised Manuscript Received June 12, 2007

ABSTRACT: Hyperbranched polyethylenes containing covalently tethered polyhedral oligomeric silsesquioxane (POSS) nanoparticles were synthesized in this work by chain walking ethylene copolymerization with a POSS macromonomer bearing a polar acrylate group, acryloisobutyl-POSS. The unique hyperbranched chain topology of these polymers was achieved owing to the chain walking mechanism of the Pd−diimine catalyst, [(ArN═C(Me)−(Me)C═NAr)Pd(CH_3)(N≡CMe)]SbF_6 (Ar = 2,6−(iPr)$_2$$C_6H_3$). Regardless of its bulky structure and polar nature, the acryloisobutyl-POSS macromonomer was successfully copolymerized to give a range of POSS−ethylene copolymers with the POSS macromonomer content up to 35 wt %. A systematic study of the effects of covalent POSS incorporation on the polymer properties was undertaken using techniques including gel permeation chromatography with on-line viscometry (GPC-VIS), X-ray diffraction (XRD), differential scanning calorimetry (DSC), thermogravimetric analysis (TGA), and rheometry. It was found from GPC-VIS measurements that the covalent incorporation of the high-mass POSS nanoparticles reduces significantly the intrinsic viscosity of the copolymers compared to homopolyethylenes of the same molecular weight, owing to the highly compact spherical cage structure of the POSS nanoparticles. Thermal studies confirm that the POSS incorporation enhances significantly the thermal oxidative stability of the polymers in air, and the copolymer glass transition temperature increases with POSS macromonomer content. The XRD study showed aggregation of POSS nanoparticles in the copolymers, leading to the formation of crystalline POSS domains. Rheological measurements demonstrate that the covalently tethered POSS nanoparticles greatly reinforce polymer rheological properties. In particular, gel-like rheological behavior was observed in the POSS copolymers. This gelation behavior is attributed to the aggregation/interactions of POSS nanoparticles, which lead to the construction of a physical network system throughout the polymer nanocomposite materials.

Introduction

Being a novel family of functional inorganic nanofillers of unique structural features and superior properties, polyhedral oligomeric silsesquioxane (POSS) has received extensive research attention as a nanoscale building block for the construction of hybrid polymer nanocomposite materials.[1−3] A typical POSS nanoparticle has a cubic inorganic Si_8O_{12} core surrounded by eight organic corner groups as shown in Scheme 1a and has a particle size of about 1.5 nm. The eight organic corner groups can be functionalized with a variety of organic substituents. Commonly, one of them is functionalized with a polymerizable or reactive group (e.g., acrylate group in Scheme 1a), while the others are designed to have identical nonreactive groups (isobutyl group in Scheme 1a).[1−3] With this unique structure, POSS molecules can be applied as macromonomers in various copolymerization systems to prepare a novel family of nanoscale-structured hybrid copolymers covalently tethered with POSS nanoparticles. It has been found in a great number of studies that such covalent POSS incorporation can significantly enhance thermal and mechanical properties of polymer materials.[3]

A variety of polymerization strategies have been developed in the past years for the synthesis of various POSS-incorporating polymers, such as polyolefins,[4−9] polynorbornenes,[10] styrenics,[11−15] acrylics,[16−20] polysiloxanes,[21,22] epoxies,[23−26] polyurethanes,[27,28] polyimides,[29,30] etc. The strategies include coordination polymerization,[5−7,11] ring-opening metathesis polymerization,[8−10] conventional free radical polymerization,[13,14,16,19,20] living/controlled radical polymerization,[17,18] anionic polymerization,[12] condensation polymerization,[22−30] etc. Recent review papers [1−3] summarize these synthetic strategies. With respect to polyolefin POSS copolymers, which is to our primary interest, however, only very limited investigations have been reported in the literature, and olefin copolymerization with POSS macromonomers still remains in an early stage of development.[6] The selection of appropriate transition-metal catalysts has been found to be critical for the successful incorporation of a POSS macromonomer into the polyolefin backbone. Moreover, nonpolar POSS macromonomers were usually chosen in the literature for copolymerization with olefins owing to the high oxophilicity of most olefin polymerization catalysts. With heterogeneous Ziegler−Natta catalysts, Schwab et al.[4] found that POSS macromonomers with alkenyl functionalities (propenyl and octenyl) could not be copolymerized with 1-hexene due to the steric resistance at the catalyst center. On the contrary, homogeneous metallocene catalysts have been found effective in copolymerizing a POSS macromonomer bearing a decenyl functionality with ethylene and propylene.[5] Coughlin et al.[6] found POSS−norbornene macromonomer could also be copolymerized with ethylene and propylene using a metallocene

* Corresponding author: e-mail zye@laurentian.ca; Fax 1(705) 675-4862.
[†] School of Engineering.
[‡] Department of Chemistry and Biochemistry.

10.1021/ma0706733 CCC: $37.00
Published on Web 07/28/2007

Scheme 1. Structure of (a) Acryloisobutyl-POSS Macromonomer and (b) Pd−Diimine Catalyst Used in This Work

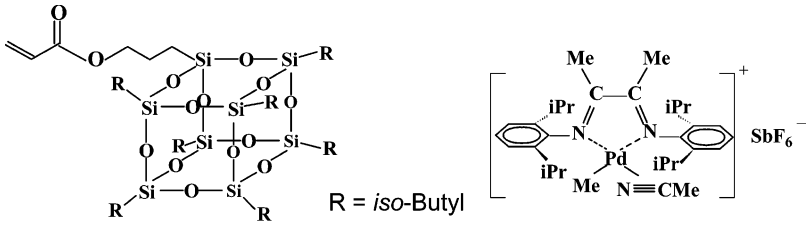

(a) Acryloisobutyl-POSS (**1**) (b) Pd-diimine catalyst (**2**)

catalyst to give high molecular weight copolymers with the POSS content up to 73 wt %.

Chain walking Pd−diimine catalysts represent a new class of olefin polymerization catalysts recently developed by Brookhart et al.[31,32] These catalysts possess the unique chain walking mechanism and allow the synthesis of highly branched polyethylenes with tunable chain topologies ranging from dendritic to hyperbranched and linear structures from a single ethylene stock.[33−35] Unlike the common strategies for the synthesis of topology-controlled polymers (such as dendrimers and hyperbranched polymers), where specially designed multifunctional monomers are required for achieving a desired chain topology, the control over polymer chain topology in this strategy is accomplished through the chain walking late-transition-metal catalysts with simple ethylene as the monomer.[33,34] In addition, owing to their significantly reduced oxophilicity, Pd−diimine catalysts allow the first successful copolymerization of ethylene and other olefins with polar functional vinyl monomers, particularly with acrylate-type functional monomers.[36,37]

In this work, we report the first investigation of the copolymerization of ethylene with a POSS macromonomer bearing an acrylate functionality, acryloisobutyl-POSS (**1**, shown in Scheme 1a), using a chain walking Pd−diimine catalyst (**2**, shown in Scheme 1b). We demonstrate that, regardless of its bulky structure and polar nature, this functional POSS macromonomer can be successfully copolymerized with ethylene by chain walking polymerization, leading to the one-pot preparation of a series of hyperbranched polyethylenes covalently tethered with inorganic POSS nanoparticles. The unique reinforcing effects of POSS nanoparticles on the properties of the hyperbranched polymer nanocomposites, such as thermal and rheological properties, were systematically investigated using techniques including X-ray diffraction (XRD), differential scanning calorimetry (DSC), thermogravimetric analysis (TGA), and dynamic oscillation rheometry.

Experimental Section

Materials. All manipulations involving air- and/or moisture-sensitive compounds were carried out in a N_2-filled drybox or using Schlenk techniques. The POSS macromonomer, acryloisobutyl-POSS (**1**), was purchased from Hybrid Plastics Inc. and was used as received. The Pd−diimine catalyst (**2**), [(ArN═C(Me)−(Me)C═NAr)Pd(CH_3)(N≡CMe)]SbF_6 (Ar = 2,6−(*i*Pr)$_2$$C_6H_3$), was synthesized according to the literature procedure.[31] Ultrahigh-purity N_2 and polymer-grade ethylene (both from Praxair) were purified by passing through 3A/5A molecular sieve and Oxiclear columns to remove moisture and oxygen, respectively, before use. Other chemicals, including anhydrous dichloromethane, petroleum ether (ACS regent grade), toluene (ACS regent grade), methanol (ACS regent grade), neutral alumina (∼150 mesh), and silica gel (grade 12, 28−200 mesh), were obtained from Aldrich and were all used as received.

Ethylene Homopolymerization and Homopolymer Purification. Ethylene homopolymerization was carried out under 1 atm ethylene pressure in a 500 mL jacketed glass reactor equipped with a magnetic stirrer. In a typical run, the jacketed glass reactor was first oven-dried, subsequently purged at least three times with ethylene, and then pressurized with 1 atm of ethylene. Subsequently, 40 mL of anhydrous CH_2Cl_2 was added into the reactor. The reactor temperature was then maintained by passing a water/ethylene glycol mixture through the jacket using a circulating bath set at the desired polymerization temperature. After thermal equilibrium for 10 min, 10 mL of the catalyst solution containing 0.1 mmol of Pd−diimine catalyst (**1**) in CH_2Cl_2 was injected into the reactor to start the polymerization. After 24 h, the polymerization was terminated by venting the reactor. The solvent was subsequently evaporated to recover the oily polymer product.

In order to remove the catalyst residue remaining in the polymer, the oily polymer product was redissolved in petroleum ether, and the solution was passed through a short column packed with neutral alumina and silica gel. The purified homopolymer was obtained by precipitation in methanol. It was dried under vacuum at room temperature for 2 days and then weighed.

Copolymerization of Ethylene with the POSS Macromonomer. Copolymerization of ethylene with the POSS macromonomer was carried out in a 500 mL jacketed glass reactor equipped with a magnetic stirrer in a similar manner as ethylene homopolymerization. In a typical copolymerization run, a prescribed amount of the POSS macromonomer was dissolved in 40 mL of anhydrous CH_2Cl_2 and then injected into the reactor, which had been previously oven-dried, purged, and filled with ethylene at 1 atm. The temperature of the reactor was then maintained by passing a water/ethylene glycol mixture through the jacket using a circulating bath set at a desired temperature. After thermal equilibrium, 10 mL of the catalyst solution containing 0.1 mmol of Pd−diimine catalyst (**1**) in CH_2Cl_2 was injected into the reactor to start the polymerization. After 24 h, the reactor was vented. CH_2Cl_2 was evaporated to recover the oily polymerization product.

Copolymer Separation and Purification. An extensive dissolution/precipitation method was used to remove the unreacted POSS macromonomer from the copolymer. The dried polymer product obtained above was redissolved in about 15 mL toluene. Then ∼8 mL of methanol was added under vigorous stirring to precipitate the copolymer out. The POSS macromonomer was found to be soluble in a 2:1 (v/v) toluene/methanol mixture. After precipitation, the solvent layer was decanted. The dissolution/precipitation procedure was repeated twice. The sticky copolymer was next redissolved in petroleum ether, and the polymer solution was passed through a short column packed with neutral alumina and silica gel to remove any Pd−diimine catalyst residue. The copolymer was finally recovered by precipitation in methanol and was dried under vacuum at room temperature for 2 days.

Preparation of Physical Blends of Homopolyethylenes with the POSS Macromonomer. Prescribed amounts of the desired homopolyethylene and the POSS macromonomer were dissolved and mixed well in a small amount of CH_2Cl_2. The CH_2Cl_2 was evaporated and the physical blend was then dried over night in a vacuum oven at room temperature.

Characterization and Analysis. Proton nuclear magnetic resonance (^{1}H NMR) spectra of the POSS macromonomer and polymers were obtained on a Varian Gemini 2000 200 MHz spectrometer at ambient temperature. Deuterated chloroform ($CDCl_3$) was used as the solvent for all the samples for NMR measurement.

Table 1. Polymerization Conditions and Some Structural Properties of the Polymers

		POSS macromonomer				POSS macromonomer content in copolymer[c]				
entry	sample	feed (g)	conc (M)	temp[a] (°C)	polymer obtained[b] (g)	mol %	wt %	SCB[c] per 1000C	M_w[d] (kg/mol)	PDI[d]
1	PE1	0	0	15	12.5	0	0	102	73	1.6
2	POSSPE1	10	0.22	15	1.2	0.39	12	107	63	1.5
3	POSSPE2	20	0.44	15	6.1	1.0	25	121	189	3.8
4	PE2	0	0	25	9.7	0	0	102	81	1.5
5	POSSPE3	5	0.11	25	3.0	0.21	7	99	79	1.4
6	POSSPE4	10	0.22	25	1.5	0.52	15	102	85	1.5
7	POSSPE5	20	0.44	25	2.8	1.2	29	105	52	1.4
8	PE3	0	0	35	8.0	0	0	102	62	1.4
9	POSSPE6	10	0.22	35	1.3	1.5	33	108	52	1.4
10	POSSPE7	20	0.44	35	4.4	1.6	35	116	63	1.3

[a] Other polymerization conditions: solvent, CH_2Cl_2; total reaction volume, 50 mL; Pd−diimine catalyst amount, 0.1 mmol; ethylene pressure, 1 atm; polymerization time, 24 h. [b] The amount of polymer obtained after extensive separation and purification. [c] Determined using ^{1}H NMR measurement in $CDCl_3$ at ambient temperature. [d] Determined using GPC-VIS measurement in THF at 30 °C.

Differential scanning calorimetry (DSC) analysis was performed on a TA Instruments Q100 DSC equipped with a refrigerated cooling system (RCS) under a N_2 atmosphere. The instrument was operated in the standard DSC mode and was calibrated with an indium standard. A N_2 purging flow of 50 mL/min was used. Samples (∼10 mg) were heated from room temperature to 250 °C at 10 °C /min and cooled to −90 °C at 5 °C /min, and the data were then collected on the second heating ramp from −90 to 250 °C at 10 °C/min.

Thermogravimetric analysis (TGA) was performed on a TA Instruments Q50 thermogravimetric analyzer. Measurements were carried out under both N_2 and air atmospheres with a continuous gas flow of 60 mL/min. A N_2 flow at 40 mL/min was used as the balance purging gas. In a typical run, the sample (∼10 mg) was heated from 100 to 600 °C at a heating rate of 20 °C/min.

Gel permeation chromatography with on-line viscometry (GPC-VIS) was carried out at 30 °C on a Polymer Laboratory PL-GPC220 system equipped with a dual differential refractive index (dRI) and viscometer detection system. One guard column (PL# 1110-1120) and three 30 cm mixed columns (PLgel 10 μm MIXED-B 300 × 7.5 mm) were used. Tetrahydrofuran (THF) was used as the eluent at a flow rate of 1.0 mL/min. Polystyrene standards (PL EasiVials) covering molecular weights from 580 to 6 035 000 g/mol were used to calibrate the GPC system.

Wide-angle X-ray diffraction (WAXRD) was carried out on a Philips PW 1710 diffractometer with Co Kα radiation (40 kV and 30 mA, $\lambda = 1.79$ Å) at ambient temperature. The diffraction data were obtained with 2θ from 3° to 110° and with a step size of 0.02° and a counting time of 6 s.

Polymer rheological characterization was carried out on a TA Instruments AR-G2 rheometer. A 25 mm parallel plate geometry of a gap size around 1 mm was used for the measurements. The measurements were all conducted in the small-amplitude dynamic oscillation mode within the frequency range of 0.001−100 Hz. Strain sweeps were performed at 1 Hz before frequency sweeps to establish the linear viscoelastic region. The experiments were typically performed at regular 10 °C intervals within a temperature range from 15 to 65 °C.

Results and Discussion

Synthesis of POSS Copolymers and Structural Elucidation. Different from the nonpolar alkenyl and norbornenyl types of POSS macromonomers used in olefin copolymerization via metallocene catalysis in the literature,[5,6] the POSS macromonomer (**1**) bearing an acrylate polar functional group was chosen in this work for copolymerization with ethylene owing to the ability of Pd−diimine catalysts to incorporate acrylate comonomers. A series of copolymerization runs were conducted at different concentration levels of POSS macromonomer and at three different temperatures (15, 25, and 35 °C) using a chain walking Pd−diimine catalyst, [(ArN═C(Me)− (Me)C═NAr)-Pd(CH_3)(N≡CMe)]SbF_6 (Ar = 2,6−(*i*Pr)$_2$C$_6$H$_3$) (**2**). A low ethylene pressure of 1 atm was chosen for all the runs with the purpose of producing hyperbranched polymers following the chain walking mechanism of Pd−diimine catalysts.[33−35] Table 1 summarizes the copolymerization conditions for the synthesis of the three sets of POSS copolymers (POSSPE1 and POSSPE2 prepared at 15 °C; POSSPE3−POSSPE5 at 25 °C; POSSPE6 and POSSPE7 at 35 °C). For comparison purposes, three ethylene homopolymers (PE1−PE3) were also synthesized at the corresponding temperatures.

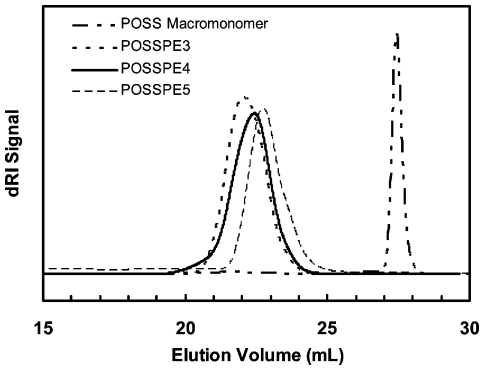

Figure 1. GPC elution traces for the POSS macromonomer and the set of copolymers synthesized at 25 °C.

Extensive purification of the POSS copolymers was carried out after copolymerization to remove the unreacted POSS macromonomer from the copolymers. The presence of physically blended untethered POSS species can also significantly affect the properties of the polymers.[38−41] A complete removal of the POSS macromonomer residue is thus critical in order for us to examine the sole effects exerted by the covalently tethered POSS nanoparticles on the polymer properties. A dissolution/precipitation method using a 2:1 (v/v) toluene/methanol mixture was used to selectively precipitate out the POSS copolymers while leaving the POSS macromonomer residue dissolved in the solvent mixture. This purification method successfully led to purified copolymers free of the POSS macromonomer residue. This was confirmed by checking the GPC elution traces of the purified copolymers. Representatively, Figure 1 demonstrates the GPC elution traces for the set of purified copolymers synthesized at 25 °C (POSSPE3−POSSPE5), together with that for the pure POSS macromonomer. Owing to its much lower molecular weight (929.6 g/mol), the POSS macromonomer has an elution peak at the elution volume

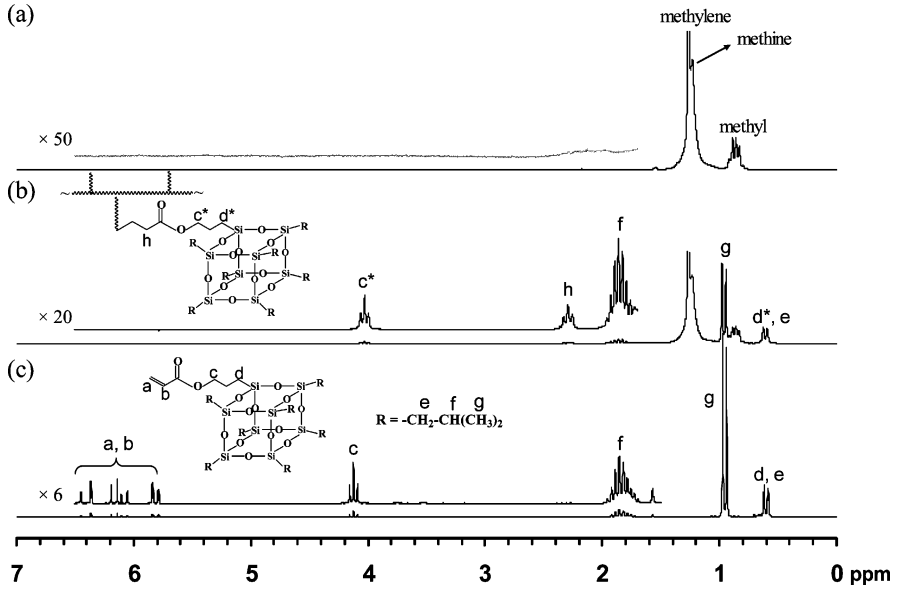

Figure 2. ^{1}H NMR spectrum of (a) PE3, (b) POSSPE7, and (c) the POSS macromonomer.

of about 27.5 mL, which is far behind those of POSS copolymers (Figure 1). Within the resolution limit of the GPC, the elution peak from the POSS macromonomer residue was not detected in all the purified POSS copolymers, confirming the absence of the unreacted POSS macromonomer in the copolymers.

The successful incorporation of the POSS macromonomer into the copolymers was confirmed by using ^{1}H NMR elucidation of copolymer structure. A representative ^{1}H NMR spectrum of a POSS copolymer, POSSPE7 prepared at 35 °C, is shown in Figure 2, along with those of the POSS macromonomer and the homopolymer, PE3 prepared at 35 °C, for the purpose of comparison. The homopolyethylene sample shows only three characteristic resonance peaks within the narrow region from 0.6 to 1.5 ppm in the ^{1}H NMR spectrum (Figure 2a), which are assigned to the methyl, methylene, and methine protons in the homopolymer. These three resonances allow the calculation of the branching density of the hyperbranched polymer, whose branching structure was generated through the chain walking mechanism of the Pd−diimine catalyst.

In the POSS copolymer, several other characteristic resonances resulting from the incorporated POSS macromonomer can be identified besides the three resonances found in the homopolyethylene. Resonance peaks (e, f, g in Figure 2b) resulting from the isobutyl group on the seven corners of the POSS cage are clearly observed in the copolymer.[17] However, vinyl resonances from acrylate group are absent in the spectrum, which suggests the covalent incorporation of the POSS macromonomer and confirms the successful removal of the unreacted POSS macromonomer through the copolymer purification procedure. At the higher chemical shift region, a triplet resonance (c* in Figure 2b) from −C(O)O−CH_2− can be observed at 4.0 ppm in the copolymer spectrum, while this methylene resonance in the POSS macromonomer is centered at ∼4.1 ppm (c in Figure 2c). This is also an evidence for the incorporation of the POSS macromonomer into the copolymer as the enchainment of the double bond shifts the position of the protons of this methylene group slightly. Moreover, a new triplet resonance centered at 2.3 ppm (h in Figure 2b), not seen in the POSS macromonomer, is found in the copolymer NMR spectrum. Integration of this triplet is approximately equal to that of the methylene resonance at 4.0 ppm (c* in Figure 2b). This triplet resonance is assigned to the methylene protons of the −CH_2−C(O)O− group. The presence of this triplet resonance suggests that the ester group of the POSS macromonomer is predominantly incorporated at the ends of branches. A schematic microstructure is shown in Figure 2b. Such a unique microstructure has been typically observed in olefin−acrylate copolymers prepared using Pd−diimine catalysts.[36,37] The mechanism leading to this microstructure has been elucidated clearly in the reports by Brookhart et al.[36,37] It is a consequence of the 2,1-insertion of acrylate comonomer into the Pd−P bond followed by rearrangement leading to the formation of a six-member stable chelate structure available for subsequent ethylene insertion.[36,37] Scheme 2 depicts the mechanism for the formation of this unique microstructure.

The above characteristic resonances resulting from the incorporated POSS macromonomer have been observed in the ^{1}H NMR spectra of all the POSS copolymers, but at different intensities. The contents of the POSS macromonomer in these copolymers were calculated on the basis of ^{1}H NMR spectra. The results are listed in Table 1. Increasing the concentration of POSS macromonomer during polymerization at each fixed temperature results in an increase in the content of the POSS macromonomer in the copolymers. At the same macromonomer concentration, increasing polymerization temperature enhances the POSS macromonomer content in the copolymers. The highest weight content of 35% with a corresponding molar content of 1.6% has been achieved with POSSPE7 prepared at 35 °C and at a POSS macromonomer concentration of 0.44 M in the polymerization system. The branching densities of the copolymers were calculated using the methyl, methylene, and methine resonances of the ethylene sequences. The results are also tabulated in Table 1. Regardless of their different polymerization temperatures and different POSS macromonomer contents, all the POSS copolymers and homopolyethylenes possess very close branching densities (∼105 branches/1000 carbons) within the limit of ^{1}H NMR measurements. The formation of the hyperbranched structure is attributed to the unique chain walking mechanism of the Pd−diimine catalyst. It should be noted that the NMR technique is ineffective in differentiating the chain topologies of the polymers due to the fact that this technique only determines the number of CH_3 groups, the branch end groups, per 1000 carbons while the

Scheme 2. Mechanism for POSS Macromonomer Incorporation in Chain Walking Copolymerization

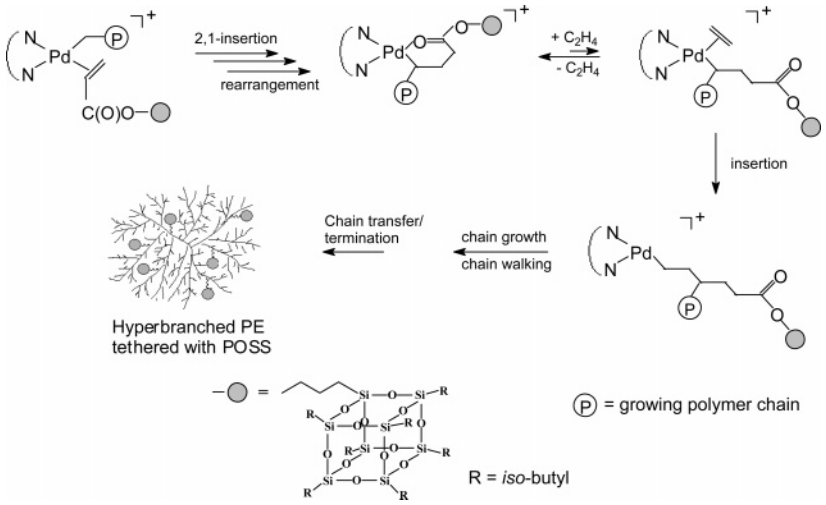

important branch-on-branch structure in these polymers cannot be detected.[33,35,42]

The physical appearance of the copolymers changes greatly with an increase of POSS macromonomer content in the copolymers. The three homopolymers, PE1−PE3, appear as transparent low-viscosity oil-like liquids. The copolymers with lower POSS content, such as POSSPE1, POSSPE3, and POSSPE4, are also oil-like liquids but with higher viscosities compared to their corresponding homopolymers. The copolymers with higher POSS content, including POSSPE2 and POSSPE5−POSSPE7, however, appear as sticky elastic solids with reduced transparency.

GPC−VIS Characterization. The GPC−VIS technique was applied to determine the average molecular weight, polydispersity, intrinsic viscosity, and chain topology information on the hyperbranched polymers synthesized in this study. In this technique, a universal column calibration curve correlating $[\eta]$-M ($[\eta]$ is intrinsic viscosity and M is molecular weight) with elution volume is constructed using known polystyrene standards. By directly measuring the intrinsic viscosity of a GPC fraction using the on-line viscometer, the molecular weight of the fraction can be precisely determined, regardless of the chain topology of the polymer, by referring to the universal calibration curve.[43] In Table 1, polymer weight-average molecular weight and polydispersity data obtained by this technique are listed. For ethylene copolymers with small-sized acrylate comonomers (such as methyl acrylate), a reduction in average molecular weight with the increase of comonomer content is usually observed.[36,37] However, for the copolymers synthesized in this study with the POSS macromonomer, we do not see such a trend based on the molecular weight data listed in Table 1. This is possibly due to the incorporation of the large-sized POSS macromonomers onto the polymer chain, which counteracts the negative effect of the comonomer incorporation on polymer molecular weight.

The GPC−VIS technique also allows us to obtain a Mark−Houwink plot ($\log[\eta]$ vs $\log M$) for the polymers, which shows the dependency of intrinsic viscosity on molecular weight of polymer fractions and provides polymer chain topology information. Figure 3a shows the Mark−Houwink plots for the three

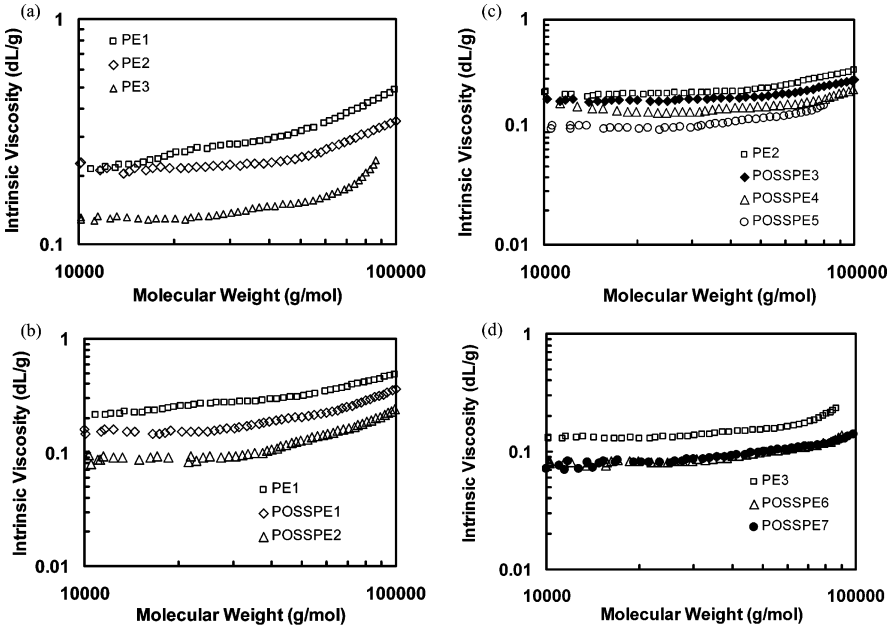

Figure 3. Intrinsic viscosity vs molecular weight plots from GPC-VIS measurements in THF at 30 °C: (a) homopolyethylenes synthesized at three different temperatures; (b) POSS copolymers synthesized at 15 °C in comparison with PE1; (c) POSS copolymers synthesized at 25 °C in comparison with PE2; (d) POSS copolymers synthesized at 35 °C in comparison with PE3.

homopolyethylenes (PE1−PE3) prepared at 15, 25, and 35 °C, respectively. From the figure, at the same molecular weight, the intrinsic viscosity value increases in the order PE3 < PE2 < PE1. In general, polymer intrinsic viscosity is related to the macromolecular coil size following the Fox−Flory equation:[44]

$$[\eta] = \Phi \frac{R_g^3}{M} \quad (1)$$

where R_g is the polymer coil gyration radius and Φ is a constant. The reduced intrinsic viscosity at a fixed molecular weight demonstrates the reduction in coil gyration radius; i.e., the polymer has a more compact chain topology. The change of intrinsic viscosity data in the three homopolymers indicates the polymer chain topology becomes more hyperbranched with an enhanced level of branch-on-branch structure from PE1 to PE3. This result is consistent with the chain walking mechanism that, at a fixed ethylene pressure, a higher polymerization temperature leads to the polymer with more hyperbranched chain topology and a lower temperature tends to linearlize chain topology.[33−35,42] Control over chain topology by tuning polymerization temperature has been reported in the literature and in our previous reports.[33−35,42]

Parts b, c, and d of Figure 3 show the Mark−Houwink plots for the three sets of polymers prepared at 15, 25, and 35 °C, respectively. For all the three sets of polymers, the incorporation of POSS macromonomer significantly reduces the polymer intrinsic viscosity compared to the corresponding homopolymer at the same molecular weight. This reduction in intrinsic viscosity is more pronounced in copolymers having a higher POSS macromonomer content. This unique effect is attributed to the highly compact structure of the tethered POSS nanoparticles. While having a high molecular weight, the POSS nanoparticle is highly compact due to its unique spherical cage structure. Its incorporation can therefore give a more compact polymer coil dimension compared to the homopolyethylene having the same molecular weight.

For linear polymers, the dependency of intrinsic viscosity on polymer molecular weight generally follows the Mark−Houwink equation with a Mark−Houwink exponent $\alpha \approx 0.70$. However, reduced α values have often been observed with topology-controlled hyperbranched polymers and dendrimers.[43] For all the homopolymers and the POSS copolymers studied here, nonlinear curves in the Mark−Houwink plots are observed, and the intrinsic viscosity of the polymers exhibits much weaker dependency on polymer molecular weight with α values typically in the range of 0.2−0.4.

XRD Characterization. Aggregation of POSS nanoparticles to form nanoscaled crystalline POSS domains has often been observed in polymers containing covalently tethered POSS nanoparticles.[7,9,10,14,24,25] This aggregation behavior is often key to the successful enhancements in the materials properties of this type of polymer nanocomposite.[7,9,10,14,24,25] Wide-angle X-ray diffraction (WAXRD) measurements at ambient temperature were conducted in this work to study the aggregation behavior in the POSS copolymers. Figure 4a shows the XRD diffraction patterns of the POSS copolymers along with those of the POSS macromonomer and a homopolyethylene sample, PE2. We also prepared four different physical blends (blends A, B, C, and D) of the POSS macromonomer and a corresponding homopolyethylene sample. The purpose is to compare the properties of these two different types of POSS-containing polymer systems. These physical blends were formulated to contain the same content of the POSS macromonomer as that

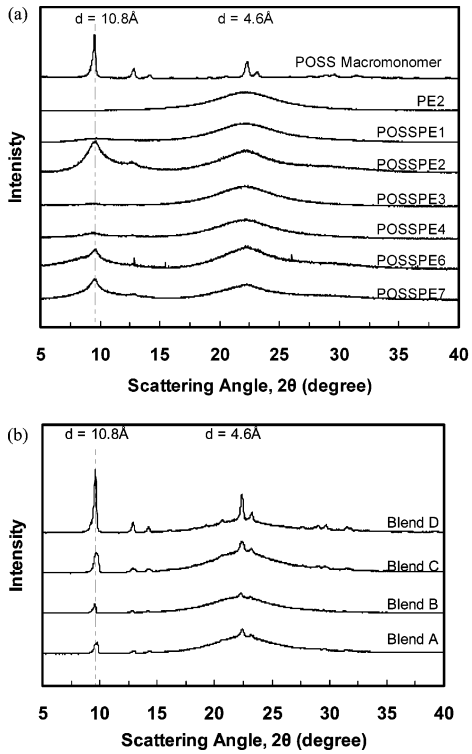

Figure 4. XRD patterns of (a) POSS copolymers in comparison with POSS macromonomer and a homopolyethylene, PE2, and (b) the physical blends of POSS macromonomer with homopolyethylenes.

Table 2. Compositions of Physical Blends of Homopolymer/POSS Macromonomer

blends	homopolymer (wt %)	POSS macromonomer (wt %)	corresponding copolymer having the same POSS macromonomer content
A	PE1 (88)	12	POSSPE1
B	PE2 (93)	7	POSSPE3
C	PE2 (85)	15	POSSPE4
D	PE3 (67)	33	POSSPE6

of the four POSS copolymers, POSSPE1, POSSPE3, POSSPE4, and POSSPE6, and the constituting homopolymer in each blend is the one synthesized at the same temperature as the corresponding POSS copolymer. The solution blending method was used for the preparation of these blends. Table 2 lists the compositions of the four physical blends prepared. In Figure 4b, the XRD diffraction patterns for these physical blends are shown.

Owing to their hyperbranched nature, the three homopolyethylene samples, PE1−PE3, are all amorphous oil-like liquids with the absence of crystalline domains. As shown in Figure 4a, only a broad amorphous halo centered at $2\theta = 22.4°$ (d = 4.6 Å) is found on the diffraction pattern of the homopolymer sample, PE2. On the contrary, the pure POSS macromonomer shows strong and sharp diffractions at 2θ's of 9.5° (d = 10.8 Å), 12.9° (d = 8.0 Å), and 22.4° (d = 4.6 Å), which are in close agreement with the literature results for isobutyl-substituted POSS structures.[10,38] Aggregation of POSS nanoparticles is evident with the POSS copolymers and is dependent on the content of the POSS macromonomer in the copolymers. From Figure 4a, POSS copolymers having low contents of the POSS macromonomer (e.g., POSSPE1, POSSPE3, and POSSPE4) show very weak almost negligible humps at $2\theta = 9.5°$ (d = 10.8 Å), which is attributable to POSS crystallites. In the copolymers with higher POSS macromonomer content, including POSSPE2, POSSPE6, and POSSPE7, the reflection peak at $2\theta = 9.5°$ becomes much sharper, but still much broader

Table 3. Crystallite Size in the POSS Copolymers and the Physical Blends

sample	crystallite size (nm)
POSSPE1	2
POSSPE2	5
POSSPE3	2
POSSPE4	4
POSSPE6	7
POSSPE7	8
POSS macromonomer	36
blend A	23
blend B	20
blend C	21
blend D	36

compared to that of the POSS macromonomer. These results show the greater tendency for POSS nanoparticles to aggregate to form crystalline domains at a higher POSS content.[7,10]

The Scherrer equation was used to estimate the apparent POSS crystallite size dimension (L) from the full width at half-maximum (fwhm) of the diffraction peak at $2\theta = 9.5°$ (d = 10.8 Å) in the XRD diffraction pattern:

$$L = \frac{K\lambda}{\beta \cos \theta} \tag{2}$$

where K is a constant ≈0.9, λ is the wavelength used (1.79 Å), and β is the fwhm (in rad) of the diffraction peak.[7] The resulting estimates of L are listed in Table 3. One can see that the POSS crystallite sizes in the copolymers are much smaller compared to that in the POSS macromonomer, and in general, the crystallite size increases with the content of the POSS macromonomer in the copolymer. Considering the size of the POSS nanoparticle is ~1.5 nm, we estimate that the crystallite involves very few POSS cages, for example, ~2 POSS cages in the cases of POSSPE1, POSSPE3, and POSSPE4.

Figure 4b shows the diffraction patterns for the four physical blends of POSS macromonomer with the corresponding homopolymer. Compared to POSS copolymers having the same POSS macromonomer content, much sharper and stronger diffraction peaks from POSS crystallites are found in these physical blends. Almost all the characteristic diffraction peaks found in the pure POSS macromonomer are present in the XRD patterns of these blends. The crystallite sizes of these blends were also estimated using the Scherrer equation and are listed in Table 3. Apparently, their crystallite sizes are much bigger compared to those of the corresponding POSS copolymers having the same POSS macromonomer content. An increase in crystallite size with the POSS macromonomer content can also be found in these blends. The difference in the XRD patterns between these two types of POSS-containing polymer systems demonstrates that much more uniform nanoscaled dispersion is achieved in the POSS copolymers, where POSS nanoparticles are covalently tethered on the polymer chains.

DSC Characterization. DSC measurements were conducted to determine the thermal transitions of the polymer samples and to study the effects of POSS incorporation on these transitions. Figure 5a−c shows DSC thermograms for the three sets of POSS copolymers. For each set, comparison is made with the corresponding homopolymer. Figure 5d shows the DSC thermograms for the four physical blends and the pure POSS macromonomer. Table 4 summarizes the DSC results for these samples.

As shown in Figure 5a−c and Table 4, the three homopolyethylenes (PE1−PE3) exhibit very close thermal behaviors with a glass-transition temperature (T_g) at −67.5 °C and a melting endotherm at $T_m \approx -34.3$ °C with $\Delta H_m \approx 9.5$ J/g. The presence of the melting endotherm indicates that these hyperbranched polymers can still crystallize, however, at a much reduced temperature and with a very low crystallinity (~3.2%). These two thermal transitions are also present in the thermograms of the POSS copolymers. However, compared to the homopolyethylenes, a slight increase in T_g is consistently found in each set of POSS copolymers, and such an increase is positively dependent on the content of the POSS macromonomer in the copolymers. For example, for the set of polymers synthesized at 25 °C, T_g increases from −67.5 °C for PE2 to −63.7 °C for POSSPE5. Such an increase in T_g has often been found in polymers containing covalently tethered POSS nanoparticles and is due to the presence of isolated bulky POSS nanoparticles, which retard the chain relaxation process.[11,13] With regards to the melting endotherm, the POSS copolymers, however, generally exhibit slightly reduced T_m and ΔH_m values compared to the homopolymers. This indicates that the POSS incorporation slightly disrupts the formation of polyethylene crystallites.[6] For the copolymers with relatively lower POSS macromonomer content, including POSSPE1 and POSSPE3, only these two thermal transitions are observed in the DSC thermograms within the temperature range from −90 to 250 °C. However, the copolymers with enhanced POSS macromonomer content have additional very weak endotherms (indicated in Figure 5 using arrows) in the temperature ranges of 0−50 and 130−150 °C. These weak transitions might be related to the melting/dissociation of the nanoscaled POSS crystallites present in the copolymers.

The DSC thermogram for the pure POSS macromonomer is shown in Figure 5d. Like the thermograms for the copolymers, this DSC thermogram was obtained on the second heating scan during DSC measurement, and only a single melting endotherm at 175 °C was observed within the temperature range up to 250 °C. While in the first heating scan (not shown in the figure) from 40 to 250 °C, a strong exotherm was detected at 164 °C together with a melting endotherm at 137 °C. The exotherm was only present in the first heating scan. It must be related to the exothermic polymerization of the acrylate POSS macromonomer. In the subsequent (second and third) heating scans, no exotherm was found, indicating the polymerization was complete in the first heating scan.

Figure 5d also compares the thermograms for the four physical blends. One can see that the two main thermal transitions related to the hyperbranched polyethylenes dominate the thermograms of the physical blends. When the POSS macromonomer content is lower than 15 wt %, the presence of POSS macromonomer seems to slightly reduce the T_g of the blends (blends A−C), and this reduction becomes more pronounced with an increase of the POSS macromonomer content (Table 4). For instance, blend C has a T_g of −68.9 °C relative to −67.5 °C for the hompolymers. This is opposite to the POSS copolymers shown above. Such a reduction in T_g due to the presence of POSS species has been observed in physically blended poly(methyl methacrylate)/POSS systems at low POSS loadings.[39] It demonstrates the plasticizing effect imposed by the molecularly dispersed POSS nanoparticles in the blends at a lower POSS macromonomer content.[39] However, for blend D having an enhanced POSS macromonomer content of 33 wt %, an elevated T_g (−65.7 °C) can be found. For blends A and B with lower POSS macromonomer content, no other thermal transitions can be found in their thermograms. But for blends C and D, an additional weak endotherm at ~180 °C can be found as shown in Figure 5d, and its intensity is higher in blend D having a higher POSS macromonomer content. This endot-

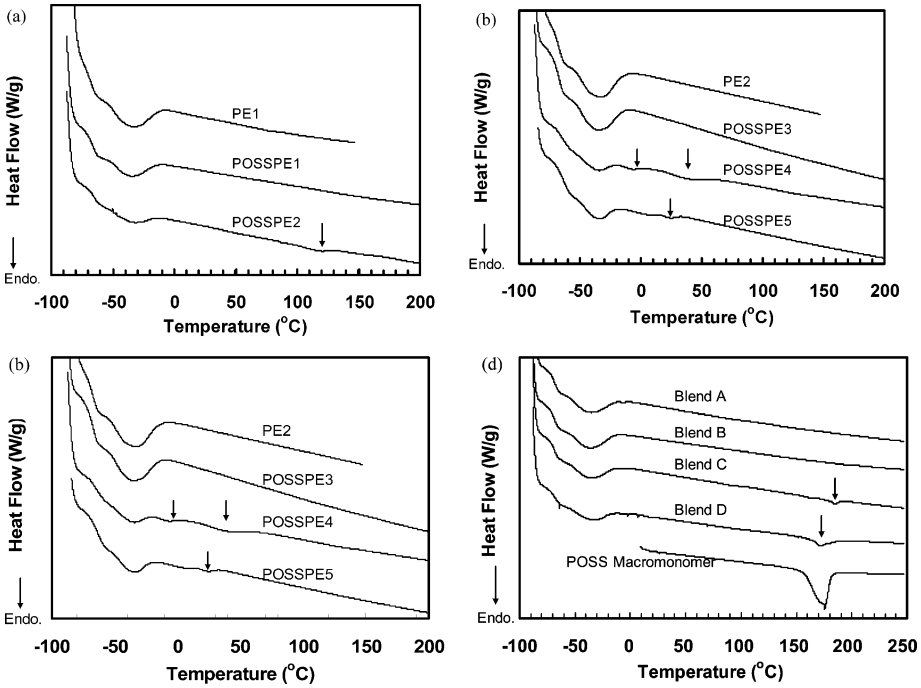

Figure 5. DSC thermograms of (a) polymers synthesized at 15 °C, (b) polymers synthesized at 25 °C, (c) polymers synthesized at 35 °C, and (d) the physical blends and the POSS macromonomer.

Table 4. DSC and TGA Data for POSS Copolymers and Polyethylene Homopolymers

				$T_{5\%}$ (°C)[b]		char yield (wt %)	
sample	T_g (°C)[a]	T_m (°C)[a]	ΔH_m (J/g)	in N_2	in air	in N_2	in air
PE1	−67.3	−34.5	9.5	388	295	∼0	∼0
POSSPE1	−66.9	−35.2	5.2	366	310	1.6	4.7
POSSPE2	−65.4	−34.2	3.6	382	366	5.6	16
PE2	−67.5	−34.3	9.5	386	304	∼0	∼0
POSSPE3	−67.0	−35.4	9.1	373	316	1.3	5.0
POSSPE4	−64.3	−35.8	4.0	370	301	1.2	5.1
POSSPE5	−63.7	−35.5	4.1	370	320	4.1	10
PE3	−67.5	−33.2	9.6	406	307	∼0	∼0
POSSPE6	−66.3	−34.5	3.8	381	336	1.6	12
POSSPE7	−63.4	−35.2	3.5	379	322	2.0	12
POSS macromonomer		175.0	13.5	282	265	15	47
blend A	−68.0	−36.3	9.9				
blend B	−68.2	−36.3	9.3				
blend C	−68.9	−36.3	8.7				
blend D	−65.7	−35.2	7.7				

[a] Determined using DSC at 10 °C/min. Weak thermal transitions are not included. [b] Thermal degradation temperature at 5% weight loss determined using TGA at 20 °C/min.

herm must be related to the melting of the POSS crystallites present in the blends. Like the POSS macromonomer, a weak exotherm at ∼167 °C due to polymerization of the POSS macromonomer was found only in the first heating scan of these two blends.

TGA Investigation. TGA measurements were carried out to investigate the effects of covalently tethered POSS nanoparticles on the thermal stability of the hyperbranched polymers. The measurements were performed on both homopolyethylenes and POSS copolymers in air and N_2 atmospheres, respectively. Figures 6 and 7 show the TGA traces of the three sets of polymers in N_2 and air atmosphere, respectively. The TGA trace of the POSS macromonomer is also shown in the figures for the purpose of comparison. The sample degradation temperature at 5% weight loss ($T_{5\%}$) and char yield data obtained from the TGA measurements are summarized in Table 4.

In both N_2 and air atmospheres, the pure POSS macromonomer exhibits lower thermal stability compared to the three homopolyethylene samples, PE1−PE3, as from Figures 6 and 7. It is relatively more stable in N_2 ($T_{5\%}$ = 282 °C) than in air ($T_{5\%}$ = 265 °C), but with a higher char yield in air as expected.[3] Based on their $T_{5\%}$ values, the three homopolyethylene samples show slightly different degradation behaviors in both N_2 and air atmospheres, possibly due to their different chain topologies. For these homopolyethylenes, the char yield is almost negligible in both N_2 and air atmospheres. The POSS copolymers show reduced thermal stability in N_2 compared to their corresponding homopolymer in each set of polymers, as is evident from the TGA curves and their reduced $T_{5\%}$ data. In each set, the POSS macromonomer content does not seem to significantly affect the value of $T_{5\%}$, and the TGA curves for the POSS copolymers are quite close regardless of their POSS macromonomer contents except for their final char yield data. The char yield is dependent on the POSS macromonomer content in the copolymers with the higher char yield found with the copolymer having a higher POSS macromonomer content.

On the contrary, the POSS copolymers exhibit enhanced thermal oxidative stability in air compared to the homopoly-

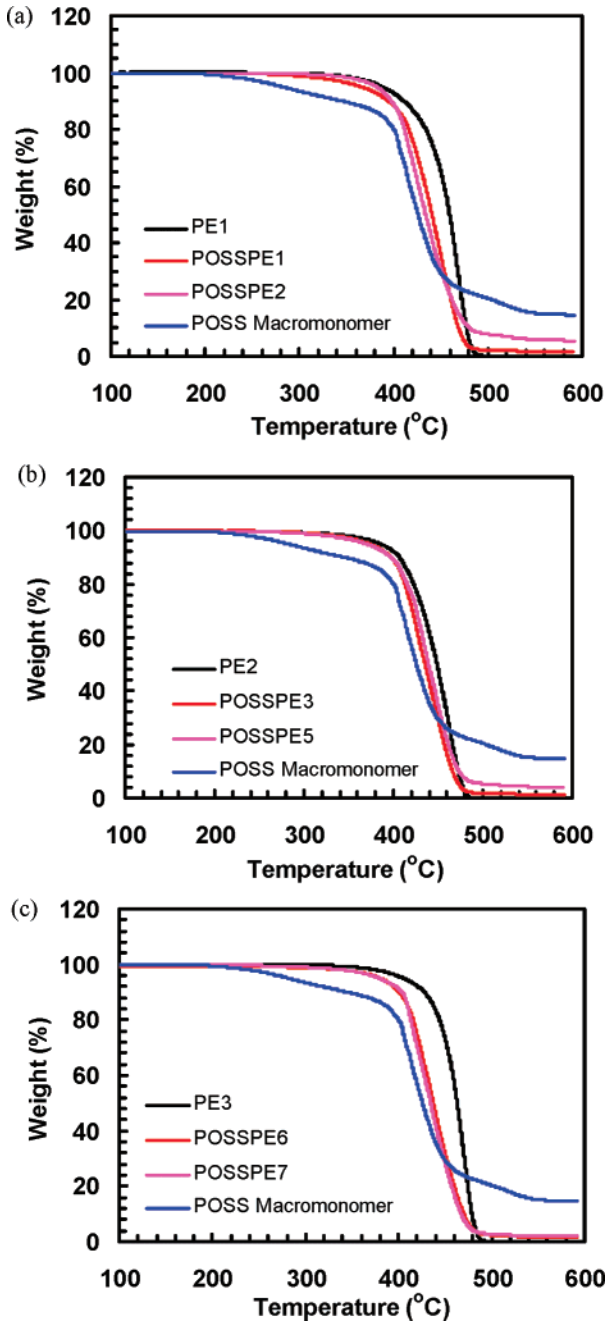

Figure 6. TGA traces in N_2 for POSS copolymers and homopolyethylenes respectively synthesized at (a) 15, (b) 25, and (c) 35 °C.

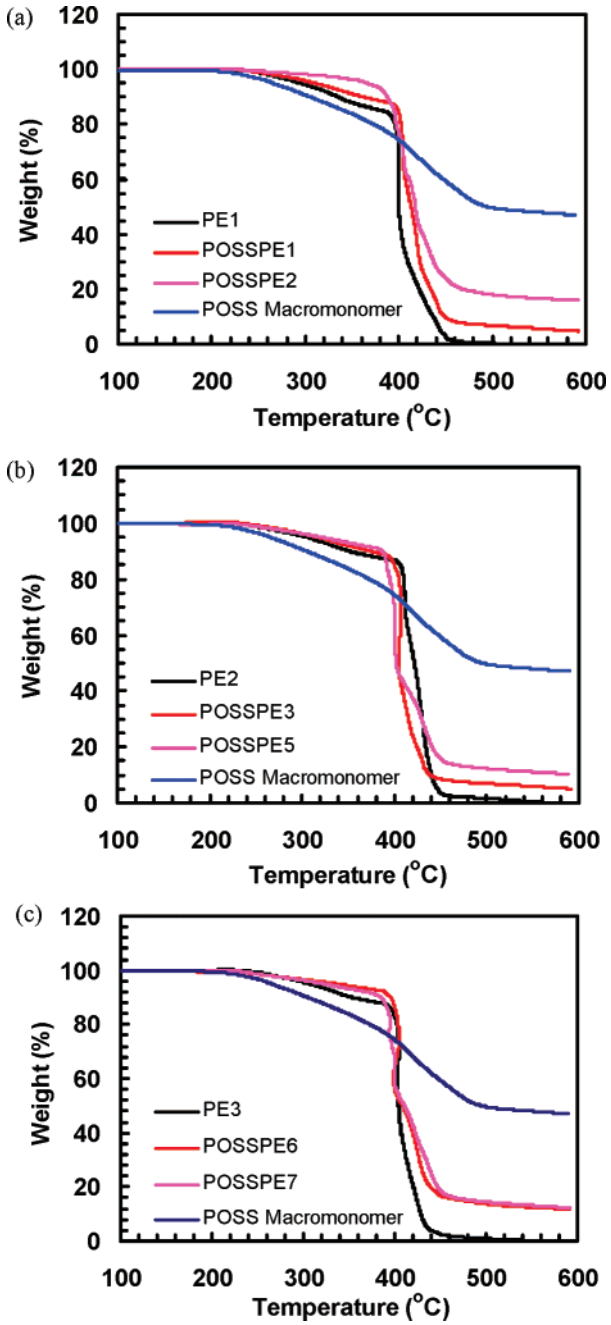

Figure 7. TGA traces in air for POSS copolymers and homopolyethylenes respectively synthesized at (a) 15, (b) 25, and (c) 35 °C.

ethylenes. As can be seen from Figure 7, in each set of polymers, POSS copolymers always have reduced weight loss compared to the homopolymer for temperatures up to 385 °C. Moreover, their thermal stability is positively dependent on the POSS macromonomer content in the copolymer with higher POSS macromonomer content leading to better stability. For example, for the set of polymers prepared at 15 °C, POSSPE1 (12 wt % POSS macromonomer) and POSSPE2 (25 wt % POSS macromonomer) have a weight loss of 11.5% and 6.8%, respectively, at 380 °C, while PE1 (homopolymer) has a weight loss of 15% at the same temperature. Meanwhile, the $T_{5\%}$ value increases from 295 °C for PE1 to 310 °C for POSSPE1 and to 366 °C for POSSPE2. Such enhanced thermal oxidative stability in air has been often found with polymers containing covalently tethered POSS nanoparticles.[5,6,8,11,25,26] One possible explanation is the formation of a thin silica layer on the surface of the polymer melt under the presence of oxygen, which serves as a barrier preventing further degradation of the polymer underneath.[6,8,11] These POSS copolymers all show higher char yield in air than in N_2, and the char yield generally increases with the POSS macromonomer content in the copolymer.

Rheological Characterization. Small-amplitude dynamic oscillatory measurements were conducted to investigate the reinforcing effects exerted by the covalently tethered POSS nanoparticles on polymer rheological properties. These measurements were all carried out in the linear viscoelastic regions of the respective polymer melts in a temperature range from 25 to 65 °C. Rheological results were obtained on the three homopolymers (PE1−PE3) and the four POSS copolymers (POSSPE1−POSSPE4). For the other POSS copolymers, measurements were not successful due to the insufficient amounts available after the other characterizations.

Figure 8 shows the master curves for the three homopolyethylene samples (PE1−PE3) at a reference temperature of

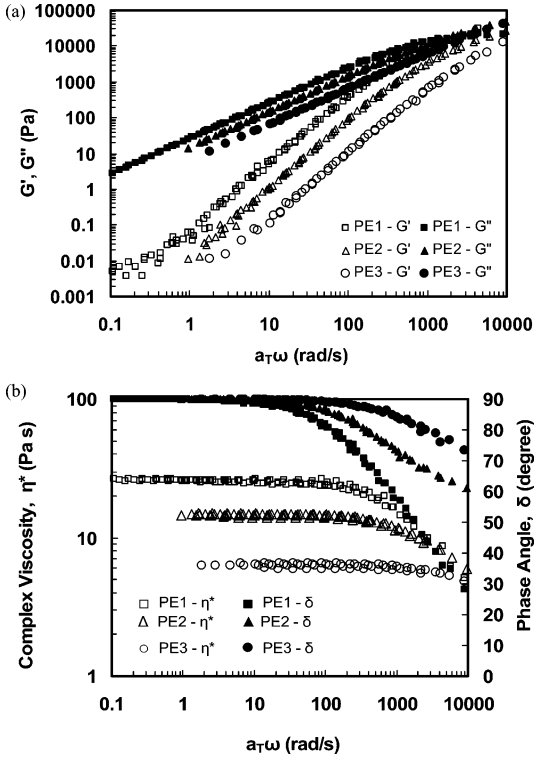

Figure 8. Master curves for the hompolyethylenes at a reference temperature of 55 °C: (a) dynamic moduli, $G'(\omega)$ and $G''(\omega)$; (b) complex viscosity and phase angle.

55 °C. The time−temperature superposition principle is applicable to these homopolymers. The topological differences among these three homopolymers having similar weight-average molecular weight and PDI can also be evidenced from these rheological results. From Figure 8a, it can be seen that both the $G'(\omega)$ and $G''(\omega)$ curves shift downward in the order from PE1 to PE3. A crossover between the $G'(\omega)$ and $G''(\omega)$ curves (at $a_T\omega \approx 2500$ rad/s) can be observed for sample PE1, while $G''(\omega)$ is always dominant over $G'(\omega)$ with no crossover for samples PE2 and PE3, showing fewer chain entanglements in PE2 and PE3. From Figure 8b, extremely low Newtonian viscosities (25 Pa s for PE1, 15 Pa s for PE2, and 6.2 Pa s for PE3) are found for all three polymers, indicating their hyperbranched chain structure. Moreover, the increase in the polymerization temperature from 15 to 35 °C results in a decrease in the Newtonian viscosity in the order PE1 > PE2 > PE3, and the Newtonian region is broadened in the same order. This is consistent with the chain walking mechanism and demonstrates the more hyperbranched chain topology and therefore fewer chain entanglements possessed by the polymer synthesized at a higher temperature.[35,42] The use of rheology as a tool to elucidate the chain topology differences among this novel range of polyethylenes by chain walking polymerization has been reported in our previous papers.[35,42]

Figure 9a shows $G'(\omega)$ and $G''(\omega)$ curves obtained at 55 °C for the set of polymers synthesized at 15 °C (PE1, POSSPE1, and POSSPE2). The covalent POSS incorporation significantly affects the $G'(\omega)$ and $G''(\omega)$ curves, and these effects are highly dependent on the POSS macromonomer content in the copolymers. At a POSS macromonomer content of 12 wt %, POSSPE1 exhibits significantly enhanced $G'(\omega)$ values at the low frequencies (up to ~10 rad/s) compared to PE1, showing the enhanced elasticity of the polymer in this frequency range.[14] However, $G'(\omega)$ values at higher frequencies and $G''(\omega)$ values within the investigated frequency range are quite close to those of PE1.

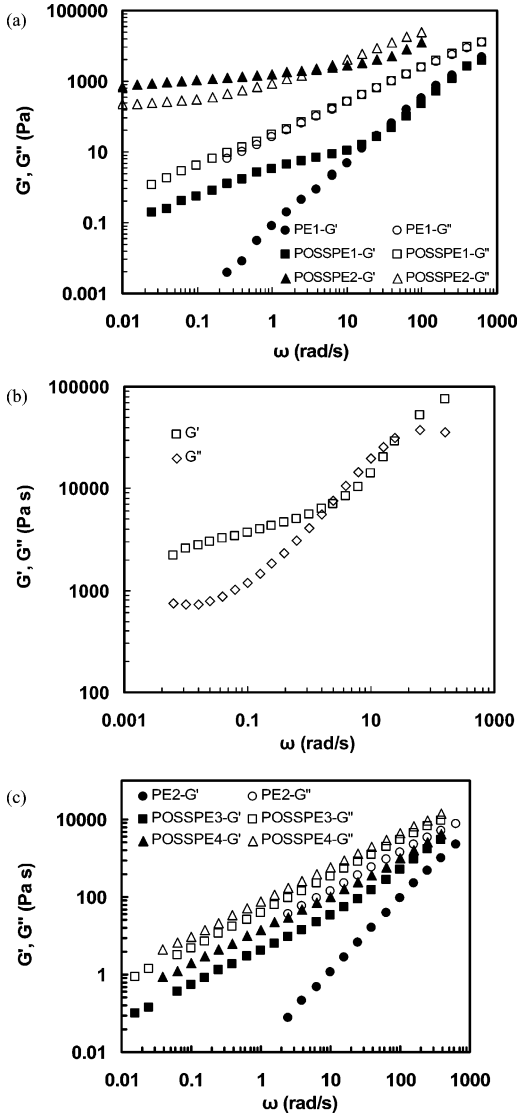

Figure 9. $G'(\omega)$ and $G''(\omega)$ curves for (a) PE1, POSSPE1, and POSSPE2 at 55 °C, (b) POSSPE2 at 25 °C, and (c) PE2, POSSPE3, and POSSPE4 at 55 °C.

Like PE1, $G''(\omega)$ is dominant over $G'(\omega)$ within the investigated frequency range and no crossover exists, indicating the polymer is still predominantly viscous. With a further increase of POSS content to 25 wt %, a drastic change in the dynamic modulus curves is incurred. Both $G'(\omega)$ and $G''(\omega)$ values are much enhanced within the whole frequency range compared to POSSPE1 and PE1.[14] A striking rubbery behavior at low frequencies with $G'(\omega) > G''(\omega)$ is observed, while it is mainly viscous with $G'(\omega) < G''(\omega)$ at the high frequencies, and a crossover point between $G'(\omega)$ and $G''(\omega)$ curves is found at ~4.0 rad/s. Moreover, the left side of the $G'(\omega)$ curve tends to reach an equilibrium value with a decrease of frequency. This is similar to the phenomenon typically observed in cross-linked polymers where $G'(\omega)$ approaches the equilibrium modulus, G_e, with a decrease of frequency.[45]

In order to further examine the $G'(\omega)$ and $G''(\omega)$ curves at even higher frequencies, Figure 9b shows the dynamic modulus curves of POSSPE2 obtained at a lower measurement temperature of 25 °C. Two crossover points can be found at this reduced measurement temperature, indicating a transition from predominantly elastic behavior at low frequencies to predominantly viscous behavior at intermediate frequencies, and back to elastic behavior at high frequencies. Similar rheological

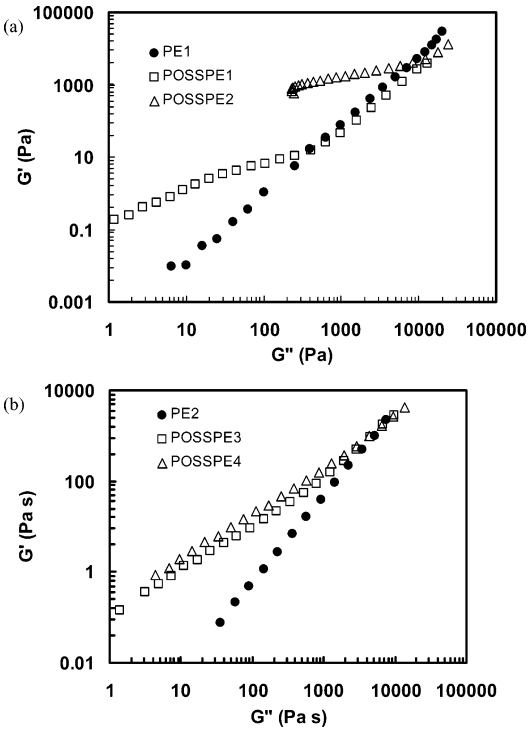

Figure 10. log G' vs log G'' plots for (a) PE1, POSSPE1, and POSSPE2 at 55 °C and (b) PE2, POSSPE3, and POSSPE4 at 55 °C.

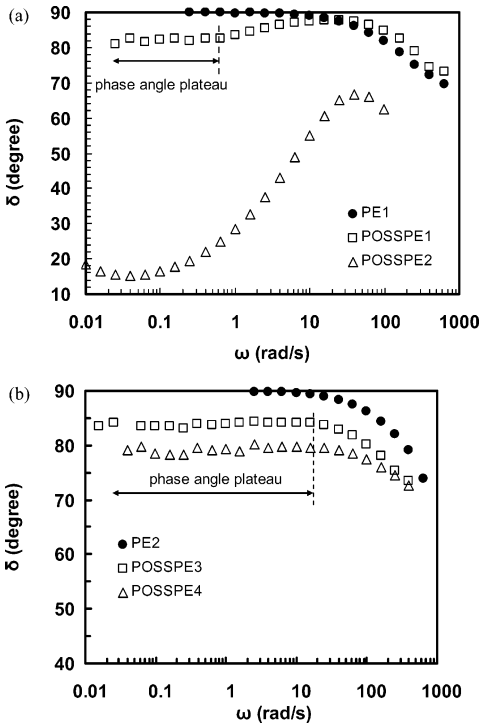

Figure 11. Phase angle curves for (a) PE1, POSSPE1, and POSSPE2 at 55 °C and (b) PE2, POSSPE3, and POSSPE4 at 55 °C.

behavior has also been found in poly(4-methylstyrene)-*co*-POSS copolymers at a high POSS content (45 wt %), and it resembles those typically observed in cross-linked polymers.[14] Figure 9c shows $G'(\omega)$ and $G''(\omega)$ curves for the set of polymers synthesized at 25 °C, including PE2, POSSPE3, and POSSPE4. Compared to the homopolymer (PE2), enhancements in both $G'(\omega)$ and $G''(\omega)$ values can be observed with the two POSS copolymers (POSSPE3 and POSSPE4), particularly in the lower frequency end. The level of enhancement is more pronounced with POSSPE4 having a higher POSS macromonomer content than POSSPE3. However, like PE2, the $G''(\omega)$ curve is always above the $G'(\omega)$ curve for these two copolymers, and no crossover exists, demonstrating the polymers are predominantly viscous within the frequency range investigated. Figure 10 compares the log G' vs log G'' curves of the two sets of polymers. For each set of polymers, an upshift in the log G' vs log G'' curve can be found with the POSS copolymers, and it is more pronounced with the copolymer having a higher POSS macromonomer content. These upshifted curves with the POSS copolymers indicate the enhanced elasticity in these copolymers compared to the homopolymer samples.[14]

Figure 11 shows phase angle (δ) curves of the two sets of polymers obtained at the measurement temperature of 55 °C. A significant reduction in phase angle and a change in the curve shape can be clearly seen in the two sets of polymers. The POSS copolymers generally exhibit a reduced phase angle compared to the homopolymers within the frequency range investigated, and the reduction is more pronounced at a higher POSS content. More interestingly, a plateau region with phase angle being independent of frequency can be observed on the left part of the phase angle curve for POSSPE1, POSSPE3, and POSSPE4. The frequency-independent phase angle plateau is typically observed in polymer gels and provides the most reliable and generally valid rheological method to determine gelation.[46−48] The presence of the phase angle plateau in these three polymers demonstrates that these POSS copolymers show physical gel-like behavior. This gel-like behavior has also been observed in polystyrenes containing covalently tethered POSS[15] and physical blends of polyethylene/POSS[40] and ethylene−propylene copolymers/POSS.[41]

The physical gelation in these copolymers should be achieved primarily by the strong aggregation or interaction among the covalently tethered POSS nanoparticles. We envisage two possible types of dispersion of the tethered POSS nanoparticles in the polymer matrix. Some POSS nanoparticles aggregate to form nanosized crystallites in the polymer matrix, as is evident in the XRD study. Some other POSS nanoparticles are dispersed in the polymer matrix in the isolated form, which is evident from the enhanced T_g of the copolymers. Interchain interactions between the isolated POSS nanoparticles can occur in the latter case.[15] These POSS aggregates/interactions can therefore serve as junction points for the construction of a physical network system throughout the polymer nanocomposite materials.[14,15] The interactions between the isolated POSS nanoparticles and the polyethylene matrix might also contribute to the network formation. However, these interactions should be much weaker compared to the strong aggregation/interaction between POSS nanoparticles.[15]

The Winter−Chambon gelation theory[49−51] is applied to analyze these physically gelled POSS copolymers. Following this theory, critical gels at the gel point exhibit simple relaxation behavior with a self-similar relaxation modulus:

$$G(t) = St^{-n} \qquad \text{for } \lambda_0 < t < \infty \tag{3}$$

where S is gel stiffness, n is the relaxation exponent and $0 < n < 1$, and λ_0 is the relaxation time characteristic of a crossover to a different relaxation mechanism. Dynamic moduli ($G'(\omega)$ and $G''(\omega)$) of a critical gel obey a scaling law with the same exponent n:

$$G'(\omega), G''(\omega) \propto \omega^n \tag{4}$$

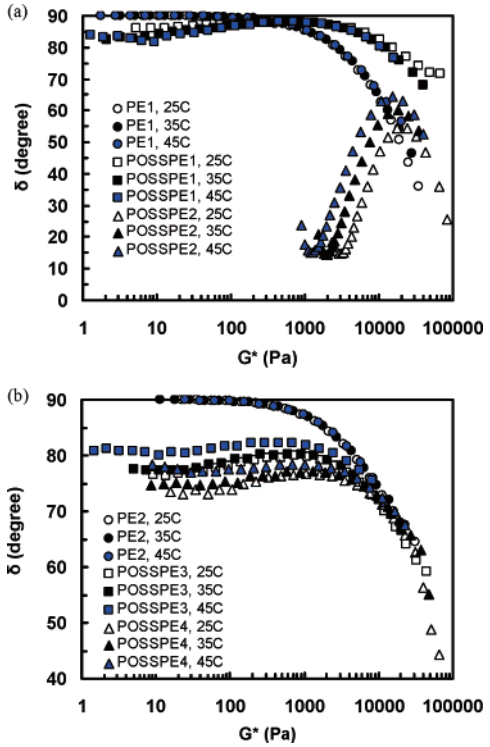

Figure 12. Van Gurp's plots for (a) PE1, POSSPE1, and POSSPE2 and (b) PE2, POSSPE3, and POSSPE4.

and they can be calculated accordingly from the relaxation modulus based on the theory of linear viscoelasticity:

$$G'(\omega) = S\Gamma(1-n)\omega^n \cos\left(\frac{n\pi}{2}\right) \tag{5}$$

$$G''(\omega) = S\Gamma(1-n)\omega^n \sin\left(\frac{n\pi}{2}\right) \tag{6}$$

where Γ is the gamma function. The ratio of the two moduli is thus independent of frequency at the gel point:

$$\tan\delta_c = \frac{G''}{G'} = \tan\left(\frac{n\pi}{2}\right) \qquad \text{for } t < 1/\lambda_0 \tag{7}$$

The dynamic modulus curves shown in Figure 9 for these three POSS copolymers indicate these polymers satisfy eq 4, the congruence condition for a gel. The value of the relaxation exponent *n* is calculated to be 0.86, 0.92, and 0.88 for POSSPE1, POSSPE3, and POSSPE4, respectively. Comparing POSSPE3 and POSSPE4, the results indicate that an increase in POSS macromonomer content results in a reduced *n* value, i.e., an enhanced gel elasticity. In addition, the phase angle plateau only exists in a limited frequency range for all the three copolymers as shown in Figure 11, indicating the crossover to different relaxation mechanism at the high-frequency end. For POSSPE2, no phase angle plateau is found in the phase angle curve shown in Figure 11a possibly due to its much higher POSS macromonomer content, leading to a post-gel behavior with significant departure from the critical gel condition.[47]

Unlike the homopolymer samples, time−temperature superposition was not applicable to these physically gelled POSS copolymers. These copolymers are therefore thermorheological complex in contrast to the thermorheologically simple homopolymers.[52] Figure 12a,b shows the Van Gurp's plots (phase angle vs log *G**) of the four POSS copolymers as well as the corresponding homopolyethylene sample. Van Gurp's plot has

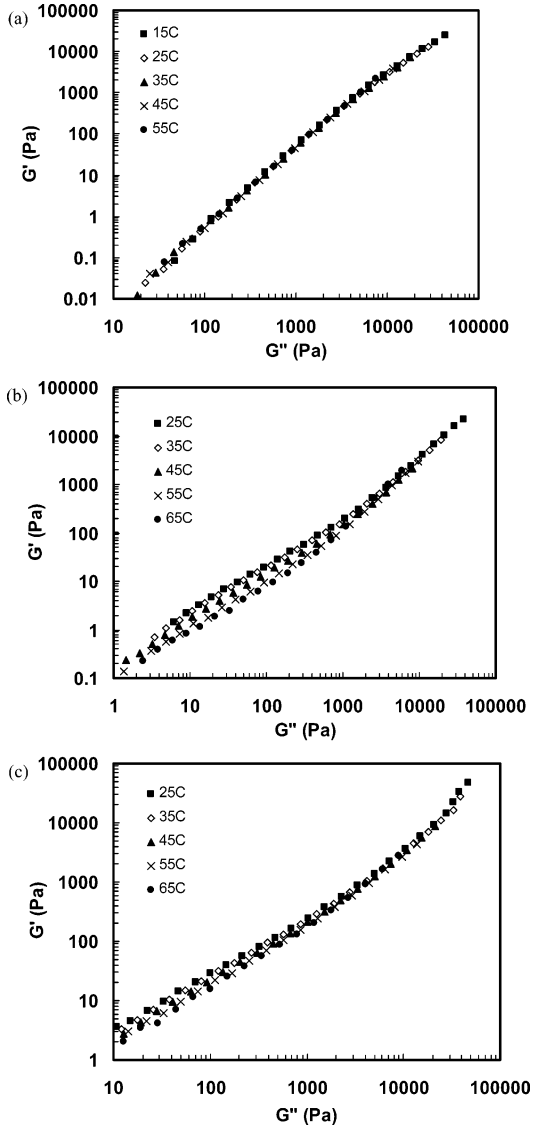

Figure 13. log *G*′ vs log *G*″ plots at different temperatures for (a) PE2, (b) POSSPE3, and (c) POSSPE4.

been shown to be a useful tool to evaluate polymer thermorheological complexity.[40,52] For thermorheological simple polymers, which obey the time−temperature superposition, the phase angle vs log *G** data measured at different temperatures should fall into a single smooth curve.[40,52] As shown in Figure 12a,b, both the homopolyethylenes, PE1 and PE2, give a smooth line. The data collected at the different temperatures for the four POSS copolymers are, however, scattered, thus violating the time−temperature superposition. For POSSPE1, POSSPE3, and POSSPE4, the phase angle plateau still exists at these different measurement temperatures (25, 35, and 45 °C). However, the phase angle value at the plateau increases slightly with the temperature increase, indicating an increase in the relaxation exponent *n* and a decrease in the gel elasticity with the temperature increase. This is different from the chemically cross-linked critical gels, which obey time−temperature superposition and have the relaxation exponent *n* independent of temperature.[47] The increase in *n* value with temperature in these physically gelled POSS copolymers suggests a slight reduction of the extent of physical cross-linking due to disassociation of some POSS aggregates/interactions at enhanced temperatures.

The temperature effects on the rheological properties of POSS copolymers were also studied using the log *G*′ vs log *G*″ plots.

The temperature dependence of log G' vs log G'' curves has been useful in determining the thermally induced order−disorder transition of block copolymers.[53] Figure 13a−c shows the log G' vs log G'' plots for the set of polymers prepared at 25 °C with data collected at several different temperatures. As expected, the homopolymer sample, PE2, exhibits a temperature-independent log G' vs log G'' curve as shown in Figure 13a. But for the two POSS copolymers, POSSPE1 and POSSPE2, a consistent downshift of the curve is observed with a temperature increase. The temperature dependence of the log G' vs log G'' curve suggests a thermally induced structural transition in the POSS copolymer systems. Considering some weak thermal endotherms observed in the temperature range from 0 to 50 °C in the copolymer DSC thermograms shown in Figure 5b, we speculate these structural transitions are the disassociation/melting of some POSS nanocrystallites resulting from the temperature increase. Such disassociation will lead to a reduced number of cross-linking junctions and, therefore, enhanced fluidity and decreased polymer elasticity. This is consistent with the downshift of the log G' vs log G'' curves shown in Figure 13b,c. A similar temperature dependency was also observed in the set of polymers prepared at 15 °C. For the purpose of brevity, the curves are not shown additionally.

Conclusion

Three sets of hyperbranched polyethylenes containing covalently tethered POSS nanoparticles were successfully synthesized by chain walking ethylene copolymerization with the acryloisobutyl-POSS macromonomer at three different temperatures (15, 25, and 35 °C) using a Pd−diimine catalyst. The study on the copolymerization system shows that the POSS macromonomer content in the copolymers is positively dependent on the POSS macromonomer concentrations during copolymerization. A ^{1}H NMR elucidation of the copolymer microstructure indicated that the POSS macromonomer is predominantly incorporated at the branch ends, which is the typical incorporation mode for acrylate-type comonomers in copolymerization with olefins by Pd−diimine catalysis.

GPC−VIS measurements show that the POSS copolymers exhibit reduced intrinsic viscosity data compared to the homopolymer fractions having the same molecular weight owing to the incorporation of the highly compact high-mass POSS nanoparticles. The reduction is more pronounced in copolymers having a higher POSS macromonomer content. On the basis of an XRD study, aggregation of POSS nanoparticles to form crystalline POSS domains has been found in the POSS copolymers and is more pronounced with an increase of POSS macromonomer content in the copolymers. Thermal studies demonstrate that the POSS copolymers have slightly increased glass transition temperature and significantly improved thermal oxidative stability in air compared to their corresponding homopolymers. Dynamic oscillation measurements show that POSS incorporation dramatically affects the rheological properties of the POSS copolymers. Generally, enhancements in both $G'(\omega)$ and $G''(\omega)$ were found in the copolymers, and they are more pronounced in copolymers having a higher POSS macromonomer content. More interestingly, gel-like behavior was observed with three POSS copolymers: POSSPE1, POSSPE3, and POSSPE4. The gelation behavior demonstrates the construction of a physical network system throughout the polymer matrix by aggregation or interaction of the POSS nanoparticles. Time−temperature superposition was found inapplicable to these POSS copolymers, possibly due to the temperature-dependent dissociation of some POSS aggregates/interactions.

Acknowledgment. The financial support from the Natural Science and Engineering Research Council of Canada (NSERC) is greatly appreciated. Z.Y. also thanks NSERC and the Canadian Foundation for Innovation (CFI) for funding research equipment and facilities.

References and Notes

(1) Li, G.; Wang, L.; Ni, H.; Pittman, C. U. *J. Inorg. Organomet. Polym.* **2001**, *11*, 123.
(2) Sanchez, C.; Soler-Illia, G. J. D. A.; Ribot, F.; Lalot, T.; Mayer, C. R.; Cabuil, V. *Chem. Mater.* **2001**, *13*, 3061.
(3) Pielichowski, K.; Njuguna, J.; Janowski, B.; Pielichowski, J. *Adv. Polym. Sci.* **2006**, *201*, 225.
(4) Shockey, E. G.; Bolf, A. G.; Jones, P. F.; Schwab, J. J.; Chaffee, K. P.; Haddad, T. S.; Lichtenhan, J. D. *Appl. Organomet. Chem.* **1999**, *13*, 311.
(5) Tsuchida, A.; Bolln, C.; Sernetz, F. G.; Frey, H.; Mülhaupt, R. *Macromolecules* **1997**, *30*, 2818.
(6) Zheng, L.; Farris, R. J.; Coughlin, E. B. *Macromolecules* **2001**, *34*, 8034.
(7) Zheng, L.; Waddon, A. J.; Farris, R. J.; Coughlin, E. B. *Macromolecules* **2002**, *35*, 2375.
(8) Zheng, L.; Farris, R. J.; Coughlin, E. B. *J. Polym. Sci., Part A: Polym. Chem.* **2001**, *39*, 2920.
(9) Zheng, L.; Hong, S.; Cardoen, G.; Burgaz, E.; Gido, S. P.; Coughlin, E. B. *Macromolecules* **2004**, *37*, 8606.
(10) Constable, G. S.; Lesser, A. J.; Coughlin, E. B. *Macromolecules* **2004**, *37*, 1276.
(11) Zheng, L.; Kasi, R. M.; Farris, R. J.; Coughlin, E. B. *J. Polym. Sci., Part A: Polym. Chem.* **2002**, *40*, 885.
(12) Cardoen, G.; Coughlin, E. B. *Macromolecules* **2004**, *37*, 5123.
(13) Haddad, T. S.; Lichtenhan, J. D. *Macromolecules* **1996**, *29*, 7302.
(14) Romo-Uribe, A.; Mather, P. T.; Haddad, T. S.; Lichtenhan, J. D. *J. Polym. Sci., Part B: Polym. Phys.* **1998**, *36*, 1857.
(15) Lee, A.; Xiao, J.; Feher, F. J. *Macromolecules* **2005**, *38*, 438.
(16) Lichtenhan, J. D.; Otonari, Y. A.; Carr, M. J. *Macromolecules* **1995**, *28*, 8435.
(17) Pyun, J.; Matyjaszewski, K.; Wu, J.; Kim, G.-M.; Chun, S. B.; Mather, P. T. *Polymer* **2003**, *44*, 2739.
(18) Ohno, K.; Sugiyama, S.; Koh, K.; Tsujii, Y.; Fukuda, T.; Yamahiro, M.; Oikawa, H.; Yamamoto, Y.; Ootake, N.; Watanabe, K. *Macromolecules* **2004**, *37*, 8517.
(19) Schwab, J. J.; Lichtenhan, J. D. *Appl. Organomet. Chem.* **1998**, *12*, 707.
(20) Li, G. Z.; Cho, H.; Wang, L.; Toghiani, H.; Pittman, C. U. *J. Polym. Sci., Part A: Polym. Chem.* **2005**, *43*, 355.
(21) Lichtenhan, J. D.; Vu, N. Q.; Carter, J. A.; Gilman, J. W.; Feher, F. J. *Macromolecules* **1993**, *26*, 2142.
(22) Seino, M.; Hayakawa, T.; Ishida, Y.; Kakimoto, M. *Macromolecules* **2006**, *39*, 8892.
(23) Choi, J.; Harcup, J.; Yee, A. F.; Zhu, Q.; Laine, R. M. *J. Am. Chem. Soc.* **2001**, *123*, 11420.
(24) Matejka, L.; Strachota, A.; Plestil, J.; Whelan, P.; Steinhart, M.; Slouf, M. *Macromolecules* **2004**, *37*, 9449.
(25) Strachota, A.; Kroutilová, I.; Kovářová, J.; Matějka, L. *Macromolecules* **2004**, *37*, 9457.
(26) Liu, H.; Zheng, S.; Nie, K. *Macromolecules* **2005**, *38*, 5088.
(27) Turri, S.; Levi, M. *Macromolecules* **2005**, *38*, 5569.
(28) Nanda, A. K.; Wicks, D. A.; Madbouly, S. A.; Otaigbe, J. U. *Macromolecules* **2006**, *39*, 7037.
(29) Leea, Y. J.; Huangb, J. M.; Kuoa, S. W.; Lua, J. S.; Changa, F. C. *Polymer* **2005**, *46*, 173.
(30) Wright, M. E.; Petteys, B. J.; Guenthner, A. J.; Fallis, S.; Yandek, G. R.; Tomczak, S. J.; Minton, T. K.; Brunsvold, A. *Macromolecules* **2006**, *39*, 4710.
(31) Johnson, L. K.; Killian, C. M.; Brookhart, M. *J. Am. Chem. Soc.* **1995**, *117*, 6414.
(32) Ittel, S. D.; Johnson, L. K.; Brookhart, M. *Chem. Rev.* **2000**, *100*, 1169.
(33) Guan, Z.; Cotts, P. M.; McCord, E. F.; McLain, S. J. *Science* **1999**, *283*, 2059.
(34) Guan, Z. *Chem.−Eur. J.* **2002**, *8*, 3086.
(35) Ye, Z.; Zhu, S. *Macromolecules* **2003**, *36*, 2194.
(36) Johnson, L. K.; Mecking, S.; Brookhart, M. *J. Am. Chem. Soc.* **1996**, *118*, 267.
(37) Mecking, S.; Johnson, L. K.; Wang, L.; Brookhart, M. *J. Am. Chem. Soc.* **1998**, *120*, 888.
(38) Kopesky, E. T.; Haddad, T. S.; Cohen, R. E.; McKinley, G. H. *Macromolecules* **2004**, *37*, 8992.
(39) Kopesky, E. T.; Haddad, T. S.; McKinley, G. H.; Cohen, R. E. *Polymer* **2005**, *46*, 4743.

(40) Joshi, M.; Butola, B. S.; Simon, G.; Kukaleva, N. *Macromolecules* **2006**, *39*, 1839.
(41) Fu, B. X.; Gelfer, M. Y.; Hsiao, B. S.; Philips, S.; Viers, B.; Blanski, R.; Ruth, P. *Polymer* **2003**, *44*, 1499.
(42) Ye, Z.; AlObaidi, F.; Zhu, S. *Macromol. Chem. Phys.* **2004**, *205*, 897.
(43) Burchard, W. *Adv. Polym. Sci.* **1999**, *43*, 113.
(44) Flory, P. J.; Fox, T. G. *J. Am. Chem. Soc.* **1951**, *73*, 1904.
(45) Ferry, J. D. *Viscoelastic Properties of Polymers*, 3rd ed.; John Wiley & Sons: New York, 1980.
(46) Schwittay, C.; Mours, M.; Winter, H. H. *Farady Discuss.* **1995**, *101*, 93.
(47) Winter, H. H.; Mours, M. *Adv. Polym. Sci.* **1997**, *134*, 165.
(48) Garcia-Franco, C.; Srinivas, S.; Lohse, D. J.; Brant, P. *Macromolecules* **2001**, *34*, 3115.
(49) Chambon, F.; Winter, H. H. *Polym. Bull. (Berlin)* **1985**, *13*, 499.
(50) Winter, H. H.; Chambon, F. *J. Rheol.* **1986**, *30*, 367.
(51) Chambon, F.; Winter, H. H. *J. Rheol.* **1987**, *31*, 683.
(52) Ye, Z.; AlObaidi, F.; Zhu, S. *Ind. Eng. Chem. Res.* **2004**, *43*, 2860.
(53) Baek, D. M.; Han, C. D. *Polymer* **1995**, *36*, 4833.

MA0706733